Xenon Reactivity Model Integrated with Point Kinetics of the SPACE Code

Seung Wook LEE a*, Kwi Seok HA a, Jong Hyuk LEE a

^aKorea Atomic Energy Research Institute, 989-111 Daedeok-daero, Yuseong-gu, Daejeon 3405, Rep. of Korea *Corresponding author: nuclist@kaeri.re.kr

*Keywords: SPACE, xenon reactivity, point kinetics, SMR, ATWS, boron-free

1. Introduction

Xenon-135 (hereafter Xe-135), one of the most significant fission products due to its exceptionally large thermal neutron absorption cross section, plays a critical role in determining reactor power. In most design basis accident (DBA) analyses for nuclear power plants, however, the reactivity effect of Xe-135 is neglected. This is because its half-life of approximately 9.2 hours leads to relatively slow transient behavior, so in DBAs that consider periods of less than 30 minutes without operator action, the reactivity change due to Xe-135 is insignificant. Furthermore, when reactor shutdown occurs in the early phase of a transient, the Xe-135 inventory increases as reactor power decreases, resulting in a negative reactivity effect. For this reason, neglecting Xe-135 in most DBA analyses for existing nuclear power plants yields conservative results.

In an Anticipated Transient Without Scram (ATWS), reactor shutdown does not occur, and the core remains in a near critical and low power state. In conventional commercial nuclear power plants, borated emergency core cooling water can be injected through the safety injection system to maintain subcriticality, eliminating the need to consider Xe-135 reactivity in safety analyses. However, the i-SMR [1] currently under development in Korea adopts a boron-free core as a top-tier requirement, making borated water injection unavailable under ATWS conditions. In i-SMR safety analyses, therefore, Xe-135 reactivity must be considered in ATWS, as well as in DBAs where core power increases and a positive reactivity effect from Xe-135 may occur. To address this, a Xe-135 reactivity model was integrated into the point kinetics model of the SPACE code, enabling its application in i-SMR safety analyses.

2. Model Development

2.1 Xenon Concentration Model

The following decay processes are associated with the production and depletion of Xe-135 [2].

$$^{135}I \xrightarrow{\beta-} ^{135}Xe \xrightarrow{\beta-} ^{135}Cs$$

Iodine (I-135) is produced by fission and depleted through β -decay (half-life: 6.7 hours), while Xe-135 is produced by both fission and the decay of I-135, and depleted through β -decay and neutron absorption.

Accordingly, the variations in the concentrations of Xe-135 and I-135 can be expressed as follows:

(1)
$$\frac{dI(t)}{dt} = \gamma_I \Sigma_f \phi(t) - \lambda_I I(t)$$
(2)
$$\frac{dX(t)}{dt} = \gamma_X \Sigma_f \phi(t) + \lambda_I I(t) - \left[\lambda_X + \sigma_{aX} \phi(t)\right] X(t)$$

where I: Iodine concentration, X: Xenon concentration, γ : yield factor of each isobar, Σ_f : macroscopic cross-section area of fission, $\phi(t)$: average thermal neutron flux, λ : decay constant of each isobar, σ_{ax} : microscopic absorption cross-section area of Xe.

2.2 Point Kinetics Model of SPACE

In the point kinetics model of the SPACE code, the neutron population density equation and the precursor concentration equation for delayed neutron production are transformed into the total fission rate equation and a modified precursor concentration equation respectively, as follows:

(3)
$$\frac{d\psi(t)}{dt} = \frac{\beta_{eff}}{\Lambda} \left\{ (r(t) - 1)\psi(t) + \sum_{i} f_{i}w_{i}(t) + S' \right\}$$

(4)
$$\frac{dw_i(t)}{dt} = \lambda_i \left[\psi(t) - w_i(t) \right]$$

where $\Psi = \Sigma_f \phi V$: total fission rate, β_{eff} : effective delayed neutron fraction, Λ : prompt neutron generation time, r: reactivity in dollar, $f_i = \beta_i/\beta_{eff}$: relative delayed neutron fraction of i-th precursor, w_i : modified number of i-th precursor λ_i : decay constant of i-th precursor, S': modified neutron source.

By integrating Eqs. (3) and (4), the total fission rate can be determined, and finally the total fission power of the core is obtained as follows:

(5)
$$P_f(t) = E_R \psi(t) = E_R \Sigma_f \phi(t) V_{core}$$

where P_f : total fission power, E_R : energy release per fission, V_{core} : total fuel volume in core.

2.3 Modified Xenon Concentration Model

Eq. (2) represents the Xe-135 concentration, i.e., the number of Xe-135 atoms per unit volume. However, as shown in Eq. (3), the final solution of the point kinetics model is the total fission rate. Therefore, for the coupling with point kinetics, Eqs. (1) and (2) are multiplied by the core volume (V_{core}) and modified as follows:

(6)
$$\frac{dI'(t)}{dt} = \gamma_{I} \Sigma_{f} \phi(t) V_{core} - \lambda_{I} I'(t)$$
(7)
$$\frac{dX'(t)}{dt} = \gamma_{X} \Sigma_{f} \phi(t) V_{core} + \lambda_{I} I'(t)$$

$$- \left[\lambda_{X} + \sigma_{aX} \phi(t) \right] X'(t)$$

where $I' = I \cdot V_{core}$: total number of I-135 in core, $X' = X \cdot V_{core}$: total number of Xe-135 in core.

The two equations above represent the rate of change of the total inventory of I-135 and Xe-135 in the core, respectively. Next, as shown in Eqs. (8) and (9), each equation is converted into a relative value with respect to the equilibrium state. The equilibrium values of Xe-135 and I-135 (X_{∞}, I_{∞}) can be obtained by setting the left-hand sides of Eqs. (6) and (7) to zero.

(8)
$$\frac{d\hat{I}(t)}{dt} = \frac{\gamma_I}{I_{\infty}} \psi(t) - \lambda_I \hat{I}(t)$$
(9)
$$\frac{d\hat{X}(t)}{dt} = \frac{\gamma_X}{X_{\infty}} \psi(t) + \lambda_I \frac{I_{\infty}}{X_{\infty}} \hat{I}(t)$$

$$- \left[\lambda_X + \sigma_{aX} \phi_0 \hat{\psi}(t) \right] \hat{X}(t)$$

where $\hat{I} = I'/I_{\infty}$, $\hat{X} = X'/X_{\infty}$, $\hat{\Psi}(t) = \Psi(t)/\Psi_0 \simeq \phi(t)/\phi_0$, ϕ_0 : initial average neutron flux specified by user, Ψ_0 : initial total fission rate.

Eqs. (8) and (9) are in a form fully compatible with the point kinetics model. By simultaneously solving these equations with the fourth-order Runge–Kutta integration method [3], the relative inventories of I-135 and Xe-135 with respect to the equilibrium state can be obtained. Accordingly, the reactivity change resulting from change of the Xe-135 inventory can also be determined.

2.4 Xenon Reactivity Model

Since Xe-135 reactivity is proportional to the Xe-135 inventory, it can be described as follows:

$$(10) \ \rho_{Xe}(t) = \rho_X \hat{X}(t)$$

The equilibrium Xe-135 reactivity, ρ_X is specified by the user through the control system of the SPACE code.

The change in Xe-135 reactivity contributing to the total reactivity that affects fission power is given as follows:

(11)
$$\Delta \rho_{Xe}^{n+1} = \rho_{Xe}^{n+1} - \rho_{Xe}^{n}$$

where n+1: current time step, n: previous time step.

3. Model Verification

The input values used for the verification of the Xe-135 concentration model and the reactivity model are shown in Table I. Users can change all values in Table I in the code input. In the verification calculations, all reactivity effects except for the scram reactivity and Xe-135 reactivity were neglected.

Table I: Input parameters for Xe transient model [4]

Variables	Units	Values	Remarks
λ_I	s ⁻¹	2.875E-5	default value
λ_X	s ⁻¹	2.092E-5	default value
γ_I	-	0.06386	default value including Te&Sb
γ_X	-	0.00228	default value
σ_{aX}	cm ²	2.7E-18	default value
ϕ_0	cm ⁻² s ⁻¹	2.5E13	assumed
$ ho_X$	\$	-0.1	assumed

3.1 Equilibrium Xenon Transient

Fig. 1 compares the analytical solutions and the calculated results for the relative inventories of I-135 (\hat{I}) and Xe-135 (\hat{X}) when the reactor is shut down under the equilibrium xenon condition. The reactor shutdown occurs two hours after the start of the calculation. In this case, the analytical solutions for the relative concentrations of two isobars after reactor shutdown are obtained by integrating Eqs. (8) and (9) with $\Psi(t)$ set to zero, as follows:

$$\hat{I}(t) = e^{-\lambda_{l}t}$$

$$\hat{X}(t) = e^{-\lambda_{X}t} + \frac{\lambda_{l}}{\lambda_{l} - \lambda_{X}} \frac{I_{\infty}}{X_{\infty}} \left(e^{-\lambda_{X}t} - e^{-\lambda_{l}t} \right)$$

After reactor shutdown, the fission rate rapidly decreases and approaches zero; therefore, I-135 decreases exponentially by decay, whereas Xe-135 initially increases during the early phase of the transient. This is because, due to the difference in decay constants between Xe-135 and I-135, the amount of Xe-135 produced from the decay of I-135 exceeds the amount depleted by its own decay. However, as the inventory of I-135, which is the source of Xe-135 production, continues to decrease, the net Xe-135 inventory starts to

decrease about 8.3 hours after reactor shutdown. The SPACE predictions successfully reproduce this behavior, with the solid lines and symbols in Fig. 1 representing the code results and the analytical solutions, respectively, showing exact agreement between the two.

Fig. 2 shows the reactivity changes predicted by the code. The blue dotted line, representing the shutdown reactivity, indicates that a value of -0.1 \$ was inserted two hours after the start of the calculation. The red dashed line represents the Xe-induced reactivity, which, following the Xe-135 concentration behavior, produces a negative reactivity effect in the early phase, but decreases below the equilibrium inventory after approximately 25 hours following reactor shutdown, thereby yielding a positive reactivity effect. Subsequently, due to the continuous decrease in Xe-135 inventory, the Xe-135 reactivity asymptotically approaches the initial equilibrium reactivity magnitude of +0.1 \\$. It is also observed that the black solid line, representing the total reactivity, closely follows the behavior resulting from the superposition of the shutdown reactivity and the Xe-135 reactivity.

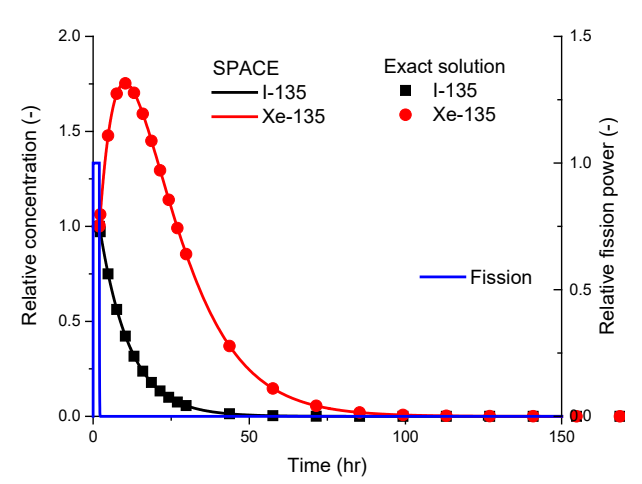


Fig. 1. Relative inventory of Xe-135 and I-135 after scram

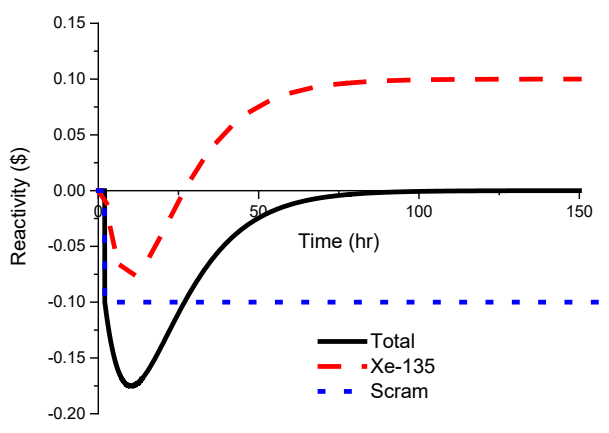


Fig. 2. Reactivity change after scram

3.2 Zero Xe Transient (Startup from Clean Core)

Fig. 3 presents a comparison between the analytical solutions and the calculated results describing how Xe-135 and I-135 reach equilibrium during constant-power operation from an initial core condition without Xe-135. In this analysis, all reactivity effects including Xe-135 reactivity were neglected and only the inventory behavior of each isobar was simulated under constant core power. Integrating Eqs. (8) and (9) with zero initial inventories for both isobars yields the analytical solutions for the relative inventories of I-135 and Xe-135 under constant reactor power, as follows:

$$\hat{I}(t) = 1 - e^{-\lambda_{I}t}$$

$$\hat{X}(t) = 1 - e^{-\lambda_{A}t} + \frac{\gamma_{I}}{\gamma_{I} + \gamma_{X}} \cdot \frac{\lambda_{A}}{\lambda_{A} - \lambda_{I}} \left(e^{-\lambda_{A}t} - e^{-\lambda_{I}t} \right)$$

where
$$\lambda_A = \lambda_X + \sigma_{ax} \phi_0$$
.

As shown in Fig. 3, the relative inventories of each isobar increase rapidly from zero at the initial time and reach 99.9% of the equilibrium inventory after approximately 72 hours. There is no significant difference in the time for each isobar to reach equilibrium. In addition, all predicted values shown as solid lines are found to match exactly with the analytical solutions represented by symbols.

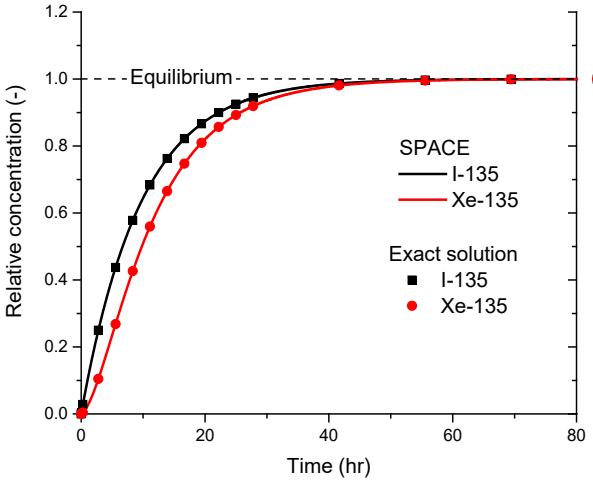


Fig. 3. Relative inventory of Xe-135 and I-135 from clean core startup

4. Conclusions

For the safety analysis of boron-free core reactors such as the i-SMR, a Xe-135 reactivity model was developed and integrated into the SPACE code in a form fully compatible with the point kinetics model. The model requires the user to specify the equilibrium Xe-135 reactivity and the initial thermal neutron flux. Verification analyses of the model were conducted for two scenarios: reactor shutdown from the equilibrium Xe-135 state and startup from an initial core without Xe-

135. In both cases, the results agreed exactly with the analytical solutions. These results confirm that the point-kinetics-coupled Xe-135 reactivity model enables accurate prediction of core power variations in ATWS scenarios for boron-free cores while accounting for Xe-135 reactivity effects.

ACKNOWLEDGEMENT

This work was supported by the Korea Institute of Energy Technology Evaluation and Planning(KETEP) and the Ministry of Trade, Industry & Energy(MOTIE) of the Republic of Korea (No. 20224B10200020) and was also supported by the Innovative Small Modular Reactor Development Agency grant funded by the Korea Government(MSIT) (No. RS-2024-00403548).

REFERENCES

- [1] Innovative Small Modular Reactor catalogue.
- [2] John R. Lamarsh, Introduction to Nuclear Engineering, 2nd edition, Addison-Wesley publishing company.
- [3] William H. Press et al., Numerical Recipes in C, Cambridge University Press.
- [4] Jams J. Duderstadt et al., Nuclear Reactor Analysis, John Wiley & Sons Inc.